Journal of Visualization, Vol. 10, No. 1 (2007)65-73

Generation of Vortices by a Streamwise Oscillating Cylinder

Alam, Md. Mahbub*[1], Fu, S.*[2] and Zhou, Y.*[1]

*1 Dept. of Mechanical Engineering, The Hong Kong Polytechnic University, Hong Kong.
*2 Dept. of Engineering Mechanics, Tsinghua University, Beijing 100084, China.

Received 16 March 2006
Revised 8 August 2006

Abstract : The wake of a streamwise oscillating cylinder is presently investigated. The Reynolds number investigated is 300, based on the cylinder diameter d. The cylinder oscillates at an amplitude of $0.5d$ and a frequency $f_e/f_s = 1.8$, where f_e is the cylinder oscillating frequency and f_s is the natural vortex shedding frequency of a stationary cylinder. Under these conditions the flow is essentially two dimensional. A two-dimensional direct numerical simulation (DNS) scheme has been developed to calculate the flow. The DNS results display a street of binary vortices, each containing two counter-rotating vortical structures, symmetrical about the centerline, which is in excellent agreement with measurements. The drag and lift on the cylinder have been examined. The time averaged drag and lift are 1.4 and 0, respectively, which are the same as those on a stationary cylinder at the same Re. However, the fluctuating drag was high, about 2.68. It has been found that, being symmetrically formed about the centerline, the binary vortices induce an essentially zero fluctuating lift, which may have a profound implication in flow control and engineering.

Keywords : Binary vortex, Streamwise oscillating cylinder, Vortex formation mechanism.

1. Introduction

The wake of an oscillating structure is frequently seen in engineering, such as flow around cable-stayed bridges, power lines, offshore structures and skyscrapers. It is therefore of both fundamental and practical significance to investigate how the wake of an oscillating cylinder behaves. Previous studies mostly focused on the transverse oscillation of one or more cylinders, perhaps because the fluctuating lift force on a structure is in many situations, say in an isolated stationary cylinder case, one order of magnitude larger than the drag force. Subsequently the lateral structural oscillation prevails against that in the streamwise direction. However, the streamwise force can be significant. Structural failure may result from synchronization between the fluid excitation force and the system natural frequency in the streamwise direction. One example is the damage of piling during the construction of an oil terminal on the Humber estuary of England in 1960s (Griffin and Ramberg, 1976). The problem of streamwise oscillation could be particularly severe when a lightly damped cylindrical structure is used in water.

There have been a limited number of studies involving a streamwise oscillating cylinder in a cross-flow. These studies have uncovered many important aspects of physics associated with a streamwise oscillating cylinder wake. For example, It is now established that the flow structure is dependent on the combination of A/d and f_e/f_s (Karniadakis and Triantafyllou, 1989), where f_e is the excitation frequency and f_s is the natural vortex shedding frequency of a stationary cylinder, A and d are the oscillation amplitude and the diameter of cylinder, respectively. Ongoren and Rockwell (1988) classified the flow structure ($A/d = 0.13 \sim 0.3$, $f_e/f_s = 0.5 \sim 4.0$) into 4 modes, i.e., S mode for the symmetric vortex formation and A-I, III, IV modes for the anti-symmetric vortex formation.

However, the cylinder oscillation amplitude previously investigated has been relatively small ($A/d \leq 0.3$). In engineering, the structural oscillation amplitude could be in the order of one cylinder diameter or even significantly larger. Xu et al. (2006) examined experimentally the flow structure behind a streamwise oscillating cylinder at a relatively large A/d (= 0.5) for f_e/f_s = 0 ~ 3.1 and observed a new flow structure, consisting of a street of symmetric binary vortices. However, due to the limitation of experiments, many aspects of the physics for this new flow structure remain to be clarified. For example, there is no information on the pressure field of the flow; the drag and lift forces associated with the flow structure is not available. The present work aims to conduct direct numerical simulation on this flow, thus complementing the experimental investigation. The numerical scheme is described in Section 2. The results are presented and discussed in Section 3. This work is concluded in Section 4.

2. Numerical Formulation

In the present numerical simulation an incompressible flow past a streamwise oscillating circular cylinder is considered. The Reynolds number, Re ($\equiv U_\infty d/\nu$, where U_∞ is the free-stream velocity, d the cylinder diameter and ν the kinematic viscosity), investigated is 300. At this Re, experimental data indicated a predominantly two-dimensional (2-D) flow (Xu et al., 2006). Therefore, a 2-D direct numerical simulation (DNS) is considered to be adequate and subsequently used for the calculation of the flow. The cylinder is allowed to oscillate, as specified by

$$x_t/d = (A/d)\sin(2\pi f_e t),\ y_t = 0, \tag{1}$$

where t is time, x_t and y_t denote the cylinder position relative to the non-oscillating case. A/d and f_e/f_s are 0.5 and 1.8, respectively, following the experimental conditions (Xu et al., 2002).

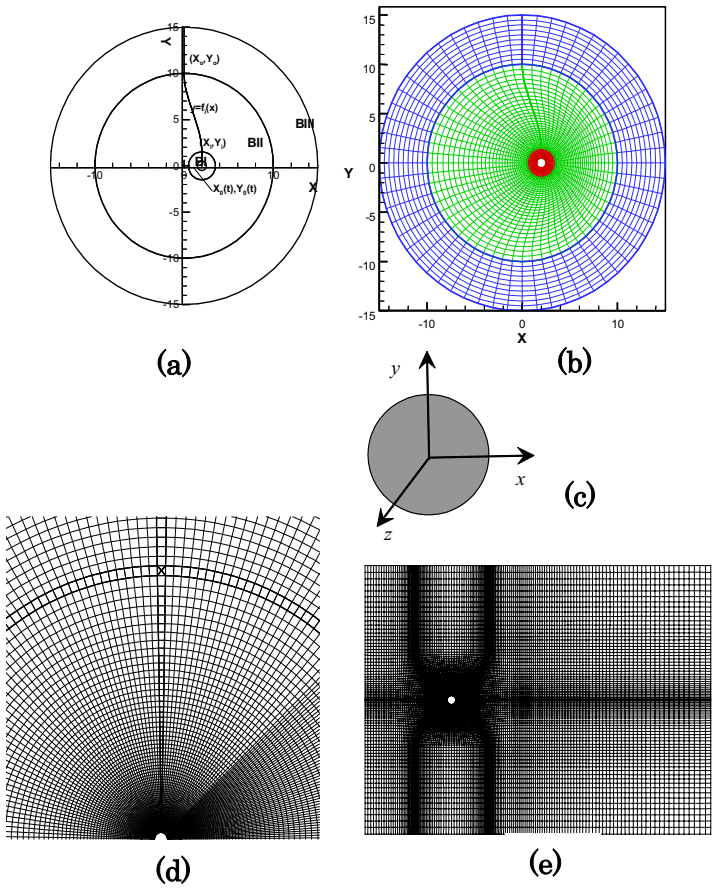

Fig. 1. (a)-(b) Three regions of the computational domain; (c) The coordinate system; (d) O-type computational grid; (e) HO-hybrid grid.

The cylindrical-polar coordinate system is used to generate the grid, providing good body-fit and accuracy. The circular computational domain is 30d, divided into inner, outer and transition regions (Figs. 1 (a)-(b)) in view of the cylinder oscillation. The inner region ($r < 1.5$) is fixed to the oscillating

cylinder, whose coordinate system is therefore non-inertial. At the boundaries of the transition region ($1.5d < r < 10d$), grid lines have been designed to ensure smoothness in terms of both grid spacing and grid velocity. This region is also in non-inertial frame with a decaying grid speed as r increases. Total mesh number is about 250 × 120 (θ by r). Note that the grid density is not uniform (Fig. 1(c)). A computational domain of 50d × 30d was tested with HO-hybrid grid system (Fig. 1(d)). The effect of the grid system on the flow structure is expectedly insignificant (not shown). The non-dimensional time step used in the calculation is $(1/f_e)/128$.

The governing equations for the flow are given by continuity and Navier-Stokes equations. With the frame of reference fixed to the oscillating cylinder in the inner region of the computational domain (Fig 1(c)), the Navier-Stokes equations may be written in terms of the curvilinear coordinates, $\xi = \xi(x, y, t)$, $\eta = \eta(x, y, t)$ and $\tau = \tau(x, y, t)$ in space and time, viz.

$$\frac{\partial u_i}{\partial \tau} + \frac{1}{J}\left[(u - x_\tau)y_\eta - (v - y_\tau)x_\eta\right]\frac{\partial u_i}{\partial \xi} + \frac{1}{J}\left[-(u - x_\tau)y_\xi + (v - y_\tau)x_\xi\right]\frac{\partial u_i}{\partial \eta} = -\frac{1}{\rho J}\frac{\partial p}{\partial \xi_j}\frac{\partial \xi_j}{\partial x_i} + \frac{\nu}{J^2}\left(\frac{\partial^2 u_i}{\partial \xi^2} + \frac{\partial^2 u_i}{\partial \eta^2}\right) \quad (2)$$

Here, the velocities u and v are still defined in the inertial Cartesian reference frame in the directions of x and y, respectively; x_τ and y_τ represents the grid speeds in the in-line and cross-flow directions defined in eq.(1). At the outer region of the computational domain the grid speeds are all zero as the inertial Cartesian grid system is adopted. In the transition region, the linear interpolation of the grid speed x_τ is employed to provide smooth variation between the inner and outer regions. Also, the variables p, ρ and J are the pressure, density and Jacobean of the two coordinate systems.

Since the present numerical simulation is based on finite-volume approach, the flow governing equations are thus further written in the integral form:

$$\frac{d}{dt}\int_V \rho\phi dV + \int_S [\rho(\boldsymbol{V} - \boldsymbol{V}_b)\phi]\cdot d\boldsymbol{S} = \int_V S_\phi dV \quad (3)$$

where ϕ =1, $\boldsymbol{V}$ denotes the continuity and momentum equations, respectively, $\boldsymbol{V}_b$ and S_ϕ represent the grid velocity vector and the corresponding source terms, respectively. No-slip boundary condition is applied to the cylinder, i.e. the fluid velocity on the cylinder surface equals to the cylinder oscillation velocity. At the exit of the computation domain, zero convection is assumed to suppress boundary disturbances, i.e.,

$$d\psi / dt + u_m d\psi / dx = 0 \quad (4)$$

where ψ can be an arbitrary transport quantity, but it particularly refers to the velocities here, and u_m represents the average u-velocity at the exit boundary (Orlanski, 1976; Saha, 2004).

3. Presentation of Results

The structural oscillation and vortex shedding may be locked in or may not. The oscillation frequency at which the lock-in occurs depends on the direction of the structural oscillation. For a laterally oscillating structure, the lock-in occurs when the oscillation frequency is close to the natural vortex shedding frequency. On the other hand, for a streamwise oscillating structure, the lock-in takes place when the oscillation frequency is near the double of the natural vortex shedding frequency. This is because the frequencies of the oscillating lift and drag on a stationary cylinder are equal to and twice the vortex shedding frequency, respectively (Nobari and Naderan, 2006). Here, the term lock-in is defined as the case where the oscillation frequency is not equal (for transverse oscillation) or twice (for streamwise oscillation) the natural vortex shedding frequency, but vortex shedding from the oscillating cylinder occurs at the excitation frequency. The present investigation focused on the streamwise locked-in state. Xu et al. (2006) observed a symmetric binary vortex street behind a streamwise oscillating cylinder (f_e/f_s = 1.74 ~ 3.08, for A/d = 0.5, Re =

500). The binary vortex formation occurred in synchronization with the oscillating cylinder. In order to compare with the experimental data, calculation was conducted for f_e/f_s = 1.8, A/d = 0.5 and Re = 300, which were close to the experimental conditions (Xu et al., 2006).

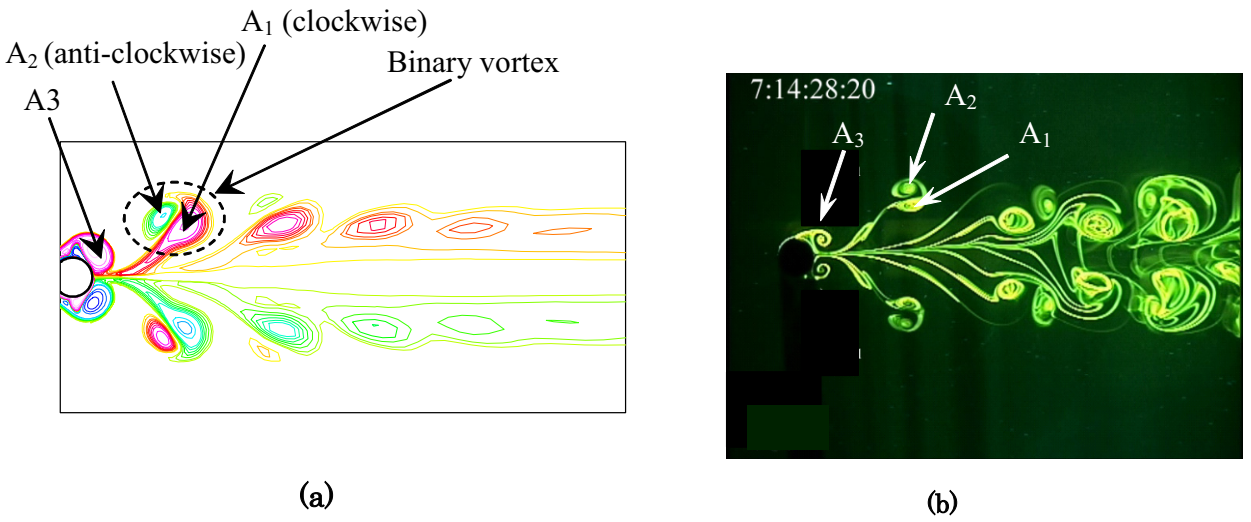

Fig. 2. Comparison between DNS result and measurements. (a) Vorticity contours from DNS, Re = 300, f_e/f_s = 1.8; (b) measured steaklines (Xu et al., 2006), Re = 500, A/d = 0.5, f_e/f_s = 1.74. Flow is left to right.

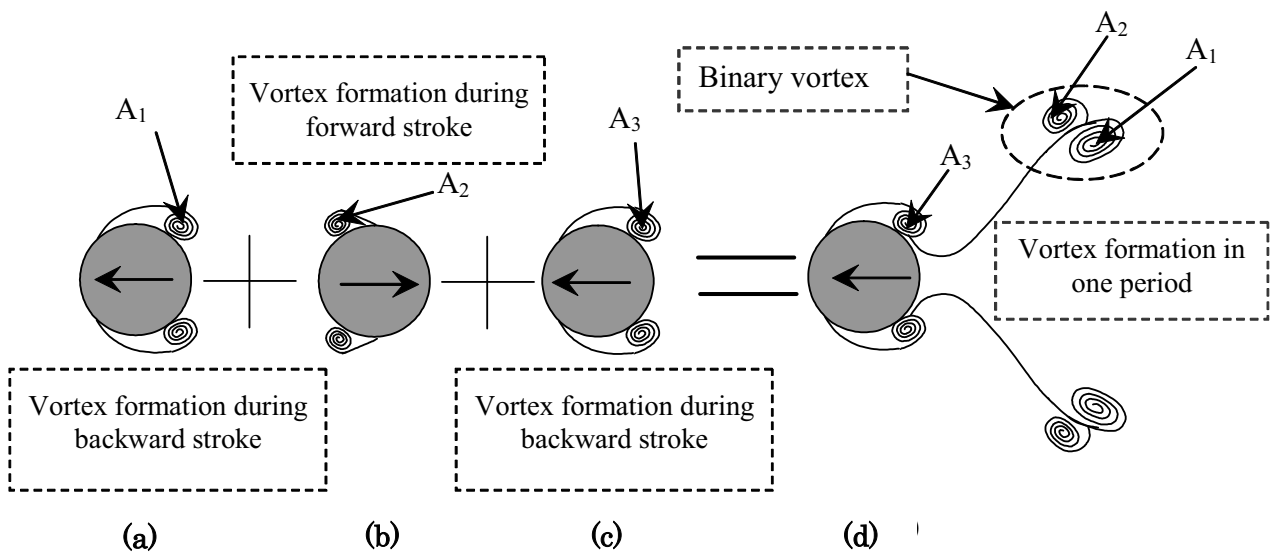

Fig. 3. Sketch of vortex formation during the backward and forward stokes of the cylinder.

The calculated vorticity contours display a symmetrically formed binary vortex street (Fig. 2(a)). Each binary vortex encloses two counter-rotating vortices. The flow structure appears the same as that (Fig. 2(b)) shown by streaklines measured using the laser-induced fluorescence (LIF) flow visualization technique (Xu et al., 2006). The contours (not shown) at different time indicate that, when the cylinder moves oppositely to the flow direction in the backward stroke, one clockwise rotating vortex, A_1, on the rear surface above the centerline forms due to the natural vortex shedding (see Fig. 3(a)). As the cylinder moves in the flow direction in the forward stroke, the fluid near the cylinder wall goes along with the cylinder under the viscosity effect, but the fluid further away now moves oppositely (right to left) relative to the cylinder. Therefore, a vortex of the anti-clockwise sense, A_2 (above the centerline), begins forming on the front surface (see Fig. 3(b)). During the forward stroke, the maximum cylinder velocity is estimated to be about 1.18 times that of fluid, implying that the cylinder moves at a higher velocity than fluid for part of the forward stroke and the relative velocity of fluid with respect to the cylinder is right to left; this could be confirmed from the induced negative time-dependent drag on the cylinder, which will be discussed later.

It can be found easily that the maximum relative velocity of fluid during the forward stroke

corresponds to an instantaneous Re_r ($\equiv U_r d/\nu$) = 54, where U_r (= $2\pi f_e A$ - U_∞ = $0.18U_\infty$) is the relative velocity of fluid with respect to the cylinder. As is well known, the creeping flow (no flow separation from the cylinder) occurs for Re < 5. At a higher Re range, i.e., 5 < Re < 30-47, steady flow separation takes place, which is accompanied by symmetrically formed twin steady vortex behind the cylinder, and alternating vortex shedding persists for Re > 30-47 (e.g., Zdravkovich, 1997; Schlichting and Gersten, 2000). It seems plausible that, once the instantaneous Re_r is in the range of 5 ~ 54 during the forward stroke, flow separation may occur, forming possibly symmetrical twin vortex on the front surface of the cylinder (Fig. 3(b)). An interesting feature seen in Fig. 2 is that A_1 is larger in size and peak vorticity than A_2. This is due to fact that the cylinder confronts a significantly higher relative flow-velocity in backward stroke than in the forward stroke.

One question may arise: why are the two same-side vortices, A_1 and A_2, close to each other behind the cylinder even though they are shed in two different cylinder oscillation strokes? During the backward stroke when vortex A_1 starts to form, the cylinder carries A_1, moves oppositely to the flow and releases it near the left end of the stroke (Fig. 3). Naturally, A_1 has relatively low absolute convective velocity. In the following forward stroke, A_1 now moves downstream. Meanwhile, vortex A_2 starts to form, which is carried by the cylinder to the right and is released when the cylinder approaches the right end of the stroke. Apparently, A_2 should have a higher absolute convective velocity than A_1. Note that the horizontal component of the viscous force in the shear layer near the cylinder is negative and positive for the backward and forward strokes, respectively (Fig. 4). This force could be also partially responsible for the decrease and increase in the absolute convective velocity of vortices A_1 and A_2, respectively. As a result, A_1 and A_2 move close to each other, forming a binary vortex just behind the cylinder.

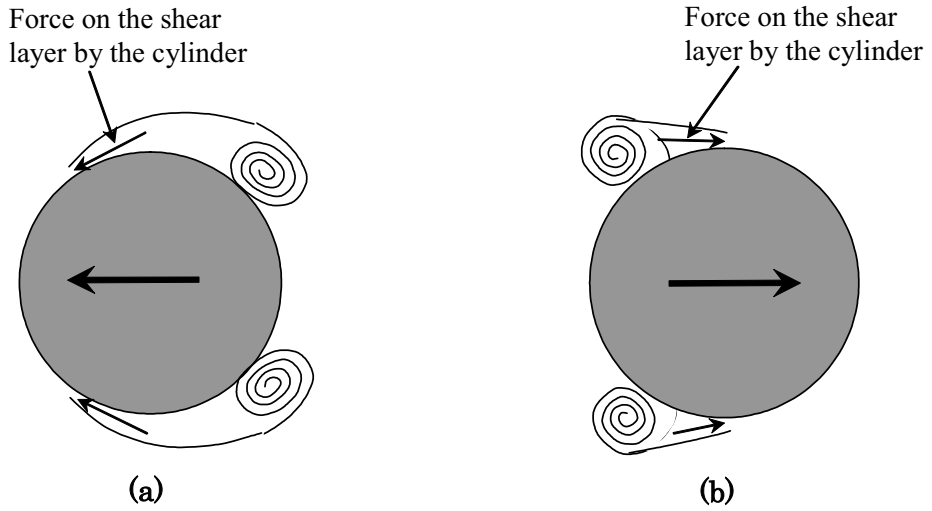

Fig. 4. The direction of the cylinder force on the shear layers during the backward and forward stokes.

As the binary vortex evolves downstream, A_2 occurs nearer to the free-stream than A_1. A_1 and A_2 are associated with negative and positive spanwise vorticity ω_z ($\equiv \partial v/\partial x - \partial u/\partial y$), respectively (Fig. 2(a)). Above the wake centerline, the mean vorticity $\overline{\omega}_z \approx -\partial\overline{u}/\partial y < 0$, which tends to cancel A_2. Alternatively, noting $\partial v/\partial x << \partial u/\partial y$ (Xu et al. 2006), $\omega_z \approx$ - $\partial u/\partial y$, we may say that A_1 ($\omega_z \approx$ - $\partial u/\partial y$ < 0) and A_2 ($\omega_z \approx$ - $\partial u/\partial y$ > 0) are under favorable and unfavorable streamwise velocity gradients, respectively. As a result, A_2 collapses rapidly, but A_1 persists longer, as shown in both DNS and experimental results (Fig. 2). Being the size and peak vorticity of A_2 smaller than those of A_1 is another cause of the rapid collapse of A_2. Similar phenomenon occurs on the other side of the cylinder simultaneously, forming symmetrical flow structure. It seems that the collapse of A_2 in the DNS result is somewhat quicker than that in the experiment. Though the basic physics of vorticity has clearly explained the cause of the rapid collapse of A_2 (which occurring in both DNS and experimental results), the cause of the quicker collapse of A_2 in the DNS than in the experiment is not clearly understood to us.

The observation from the calculated data shows extraordinary similarity to that observed in

experimental data (Xu et al., 2006). The good agreement provides a validation for the present DNS scheme. Note that the measured vortex street appears laminar at Re = 500, which is different from the DNS data (Re = 300). This should not invalidate the comparison; Zdravkovich (1997) and Griffin and Ramberg (1976) suggested that, as the oscillation of a cylinder exceeds a threshold amplitude, the oscillation amplitude and frequency may become the governing parameter of the flow regime within a certain range of the free-stream velocity, instead of Re. Note that the present A/d (= 0.5) is significantly higher than the threshold amplitude A/d = 0.07 for f_e/f_s = 1.8 (Griffin and Ramberg, 1976).

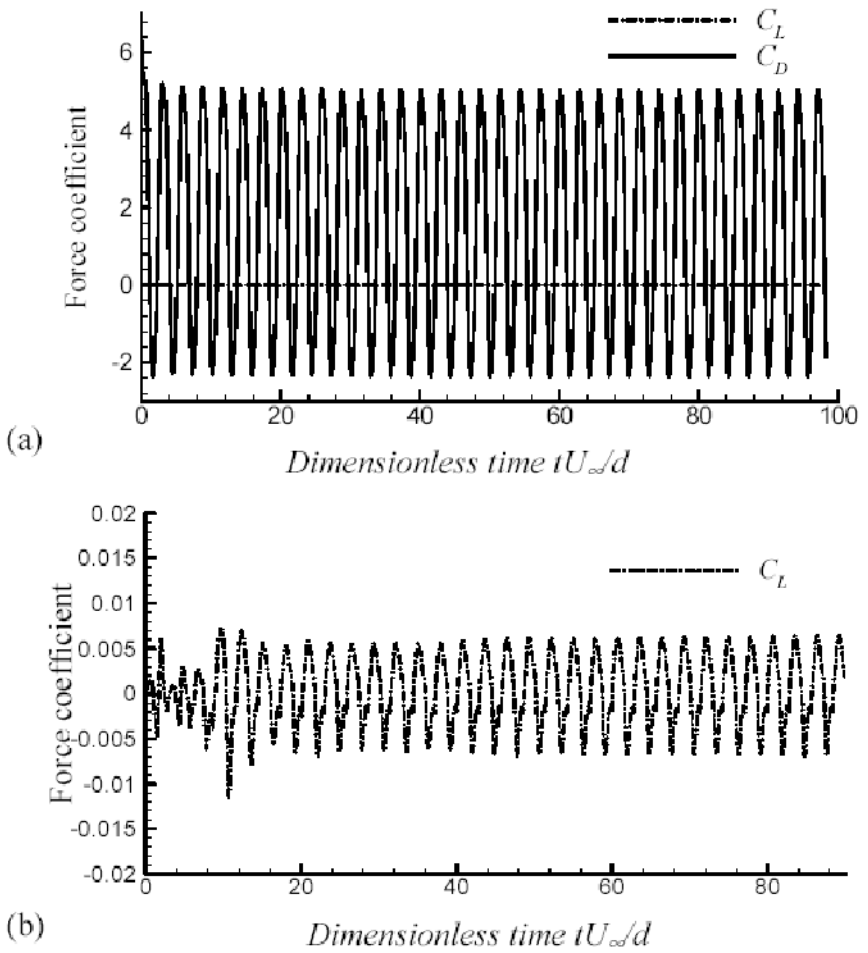

Fig. 5. Time histories of drag (upper) and lift (lower) coefficients.

In order to calculate the drag and lift coefficients, the pressure around the cylinder is obtained through the integration of the following equation,

$$\partial p / \partial n\big|_{body} = -\rho \vec{a} \cdot \vec{n} + \mu \nabla^2 \vec{u} \cdot \vec{n}\,, \tag{5}$$

where $\vec{a}$ is the acceleration of the oscillating cylinder, μ is the viscosity and $\vec{n}$ is the unit normal vector of the cylinder surface. This approach may better account for the non-inertial (added mass) and curvature effects on the pressure around the cylinder. Though the contribution of added mass effect on the drag (fluctuating) was not calculated separately, it could be mentioned that the contribution depends on f_e/f_s, and it becomes small as resonance occurs (Sarpkaya, 1979; Nishihara et al., 2005).

The first order approximation would be $\partial p / \partial n\big|_{body} = 0$. The lift and drag are obtained by integrating the pressure around the cylinder. The calculated root mean square (rms) lift coefficient $C_L^{'}$ (Fig. 5) is extremely small, about 0.005, essentially zero, which is consistent with the flow structure symmetrical about the centerline. However, the instantaneous drag coefficient C_D varies from -2.4 to 5.2 periodically. The negative C_D accounts for about 77 % in time during the forward stroke, conforming to the fact that the relative velocity of fluid with respect to the cylinder is right to left for part of the forward stroke, as discussed earlier. The rms drag coefficient $C_D^{'}$ is about 2.68,

significantly larger than that on a stationary cylinder. Two reasons account for such a large $C_D^{'}$. One is the generation of vortex A_1 on the after-body of the cylinder during the backward stroke and the other is the formation of vortex A_2 on the fore-body during the forward stroke. Symmetric periodic vortex formation should corresponds to a higher $C_D^{'}$ than periodic alternating vortex. Okajima et al. (2001) observed a large amplitude of inline oscillation of an elastic cylinder (Re = $0.8\times10^4 \sim 4\times10^4$) for the reduced velocity range of 2.5 - 3.3, corresponding to f_e/f_s = 2 – 1.5. The cylinder oscillation was attributed to the formation of symmetrical vortex shedding from the cylinder, which is consistent with the large fluctuating drag observed presently. The time-averaged drag $\overline{C}_D$ on the oscillating cylinder is estimated to be 1.4, close to that (1.37) on a stationary cylinder at Re = 300 (Nobari and Naderan, 2006).

The power spectral density functions, E_{CD} and E_{CL} (Fig. 6), of C_D and C_L both display a pronounced peak at fd/U_∞ = 0.36, which is below twice the non-dimensional frequency, 0.2, of vortex shedding from a stationary cylinder. It has been confirmed that the frequency of vortex shedding from the oscillating cylinder is identical to the oscillating frequency, that is, the vortex shedding frequency is modified and locked in with the cylinder oscillation.

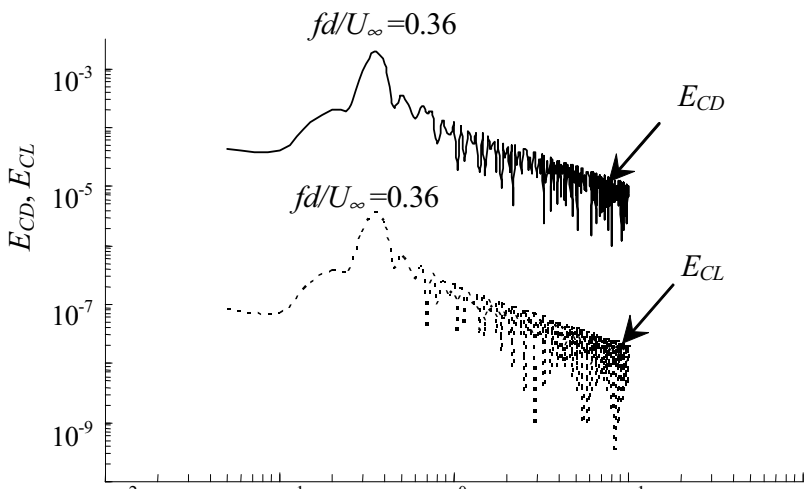

Fig. 6. Fourier spectral density functions of C_D and C_L.

In order to determine whether the lock-in is stationary or how much it is stationary, it is pertinent to analyze the time-frequency relationship of the C_D signal. The Fourier transform provides averaged spectral coefficients that are independent of time. If the Fourier transform is employed to analyze a signal, information on the dependence of frequency and power intensity on time will be lost. The wavelet analysis may be used to produce a potentially more revealing picture of the time-frequency-power localization of the signal. This technique has been used to analyze effectively the flow structures in the literature, e.g., Rinoshika and Zhou (2005a, b). Fig. 7 shows the time-frequency analysis result of the C_D signal by using Morlet wavelet with a wave number of 6. See Alam et al. 2005 for the details of the wavelet analysis. Evidently, the dominant frequency and power intensity at this frequency are unchanged along the whole signal, indicating that the flow structure generated in a period is repeated in the next period.

4. Conclusions

The flow around a streamwise oscillating circular cylinder has been investigated based on two-dimensional direct numerical simulation. The investigation leads to the following conclusions.

Firstly, the DNS data at A/d = 0.5 and f_e/f_s = 1.74 display a symmetrical binary vortex street generated by the oscillating cylinder, in excellent agreement with experimental data obtained under similar conditions. The agreement indicates that the presently developed DNS scheme can be used to calculate reliably flow around a cylinder oscillating at relatively large amplitude and

frequency ratios.

Secondly, the formation and evolution of the binary vortex has been analyzed and discussed in detail. The analysis indicates that the positive-signed structure within the binary vortex (above the centerline) should decay faster than the negative-signed structure, which is consistent with the experimental observation.

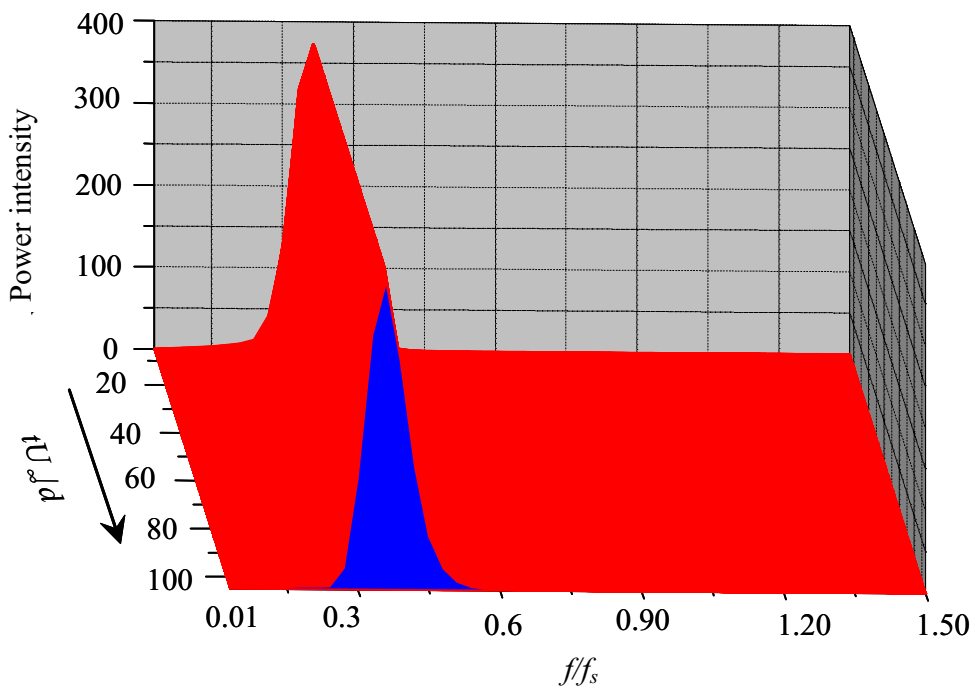

Fig. 7. Wavelet scalogram of time-dependent frequency and power spectral intensity function of the C_D signal.

Thirdly, the DNS data indicate that the time-averaged drag on the oscillating cylinder is almost the same as that on a stationary cylinder. However, the fluctuating lift coefficient approaches zero (0.005), whilst the fluctuating drag coefficient on the cylinder has been increased to 2.68. Apparently, the binary vortex street symmetrical about the centerline is responsible for the zero fluctuating lift. This observation may have a profound implication on flow control. For instance, a cylinder may be forced to oscillate longitudinally such that a downstream engineering structure, bombarded by symmetrical vortices, will experience zero fluctuating lift.

References

Alam, M. M. and Sakamoto, H., Investigation of Strouhal frequencies of two staggered bluff bodies and detection of multistable flow by wavelets, Journal of Fluids and Structures, 20 (2005), 425-449.

Griffin, O. M. and Ramberg, S. E., Vortex shedding from a cylinder vibrating in line with an incident uniform flow, Journal of Fluid Mechanics, 75 (1976), 257-271.

Karniadakis, G. E. and Triantafyllou, G., Frequency selection and asymptotic states in laminar wakes, Journal of Fluid Mechanics, 199 (1989), 441-469.

Nishihara, T., Kaneko, S. and Watanabe, T., Characteristics of fluid dynamic forces acting on a circular cylinder oscillated in the streamwise direction and its wake patterns, Journal of Fluids and Structures, 20 (2005), 505-518.

Nobari, M. R. H. and Naderan, H., A numerical study of flow past a cylinder with cross flow and inline oscillation, Computer & Fluids, 35 (2006), 393-415.

Okajima, A., Kosugi, T. and Nakamura, A., Experiments on flow=induced in-line oscillation of a circular cylinder in a water tunnel, JSME International Journal, 44 (2001), 695-704.

Ongoren, A. and Rockwell, D., Flow structure from an oscillating cylinder. Part II. Mode competition in the near wake, Journal of Fluid Mechanics, 191 (1988), 225-245.

Orlanski, I., A simple boundary condition for unbounded flows, Journal of Computational Physics, 21 (1976), 251-256.

Rinoshika, A. and Zhou, Y., Effects of Initial Conditions on a Wavelet-decomposed Turbulent Near-wake, Physical Review E, 71 (2005b), 057504, 1-8.

Rinoshika, A. and Zhou, Y., Orthogonal wavelet multi-resolution analysis of a turbulent cylinder wake, Journal of Fluid Mechanics, 524 (2005a), 229-248.

Saha, A. K., Three-dimensional numerical simulations of the transition of flow past a cube, Physics of Fluids, 16 (2004), 1630-1646.

Sarpkaya, T., Vortex-induced oscillations: A selective review, Journal of Applied Mechanics, 46 (1979), 241-257.

Williamson, C. H. K., Vortex dynamics in the cylinder wake, Annual review of Fluid Mechanics 28 (1996), 477-539.

Xu, S. J., Zhou, Y. and Wang M. H., A symmetric binary vortex street behind a longitudinally oscillating cylinder, Journal of

Fluid Mechanics, 556 (2006), 27-43.
Zdravkovich, M. M., Flow around circular cylinders Vol. 1: Fundamentals, (1997), Oxford University Press, England.

Author Profile

Md. Mahbub Alam: He served as a lecturer in the Department of Mechanical Engineering at Rajshahi University of Engineering and Technology (Bangladesh) in 1995-1998. He taught Fluid Mechanics, Engineering Mechanics and Solid Mechanics to undergraduate students. He pursued his M.Sc. and PhD degree with Prof. Hiroshi Sakamoto at Kitami Institute of Technology (Japan) during 1999-2001 and 2001-2004, respectively. After obtaining PhD degree, he has been working as a Post-Doctoral Fellow at The Hong Kong Polytechnic University since August 2004. His current research interest focuses on bluff-body aerodynamics, fluid dynamics on multiple structures, flow control, flow-induced vibrations, wavelet application in fluid mechanics and signal analysis. He published 15 journal papers and more than 20 conference papers. He has acted as a reviewer for some engineering journals.

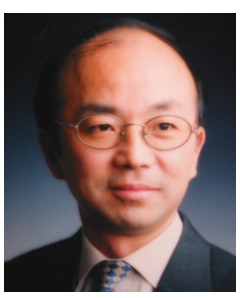

Song Fu: He received his B.Sc.(Hon) degree in Mechanical Engineering in 1983 from Imperial College London and Ph.D. degree in Mechanical Engineering in 1988 from the University of Manchester. After obtaining Ph.D. degree he joined Tsinghua University till now. He is currently a full professor and deputy dean of the School of Aerospace Engineering. His current research interests include turbulence modeling, computational fluid dynamics and turbomachinery.

Yu Zhou: He completed his PhD degree in 1992 at The University of Newcastle (Australia) and joined The Hong Kong Polytechnic University in 1995. His research interests include turbulent flows and control, flow-induced vibrations and control. He has authored or co-authored more than 200 technical papers, including more than 100 international journal and book articles, 7 being published in prestigious Journal of Fluid Mechanics. Two articles, published in Journal of Fluid Mechanics in 2001 and 2002, respectively, have been listed in the TOP 1 % MOST CITED ARTICLES within its field in 2005 by THOMSON according to Essential Science Indicators. Since 1996, he has attracted a research fund of more than 25 million HK dollars (or 3 million US dollars) from both internal and external sources and successfully supervised 7 PhD theses. Along with Dr H Li, he received 2003 VSJ Paper Award of the Visualization Society of Japan.